Numerical Analysis of o Propeller in Ground Effect

Jelena Svorcan [1]
Aleksandar Kovačević[1]
Toni Ivanov[1]
Aleksandar Simonović[1]

Detailed studies of propeller flows are regaining both interest and significance worldwide, as the number of their different design and applications (particularly for futuristic urban air vehicles) continues to grow. An additional distinctive characteristic of small-scale unmanned air vehicles (UAV) propellers is that they are meant to operate in a wide range of (previously considered atypical) operating conditions, including backward flight, flight in the vicinity of obstacles, hard/ground surfaces, etc. These specific requirements raise the issue of the effects of ground proximity on their aerodynamic performance. This paper computationally investigates flows around a small-scale, custom-made propeller in ground effect. Different ground distances are considered and novel thrust and power relations (dependencies) on them are proposed. In order to obtain sufficiently reliable and accurate results and capture the most significant flow features, Reynolds-averaged Navier-Stokes (RANS) equations are solved by finite volume method. In addition, interesting flow visualizations are presented. Although the obtained thrust trend correlates well with the conventionally used semi-empirical formula, more realistic estimations are obtained for small ground distances. Furthermore, the positive effects of ground vicinity on rotor aerodynamic performances are once again confirmed and quantified.

Key words: **propeller, turbulence, RANS, IGE.**

Introduction

NUMEROUS diverse aerial platforms, equipped with rotors that generate sufficient amounts of thrust, are designed, investigated, manufactured, and flown worldwide [1-3]. Their low cost, flexible operability and maneuverability enable a wide range of different applications, including scientific measurements, infrastructure inspection, deliveries, surveillance, crop/spray dispersion in agriculture, etc. These tasks often demand that the aircraft comes quite close to the referent surface, which may significantly affect its aerodynamic performance since the shed vortices interact with the rigid boundaries.

This flow phenomenon, when the streamtube of induced velocities formed by the rotor rotation dilates (expands) and adjusts to the surface downstream instead of narrowing, is entitled "ground effect" (IGE). It has been known and successfully modelled (firstly by simple potential flow theory and now by more complex computational models) for decades [4-6]. A rather simple expression can be used to estimate the increase of thrust T_{IGE} relative to the thrust of an isolated rotor T_{OGE} with respect to the relative distance from the ground z/R (where z is the absolute distance) at constant torque/power of an arbitrary rotor of radius R [4]:

$$\frac{T_{IGE}}{T_{OGE}} = \frac{1}{1-\left(\frac{R}{4z}\right)^2} \tag{1}$$

It may be observed that Eq. 1 doesn't take into account any specific geometric features of the inspected rotor. Nowadays, with the increased availability and constant advancement of CFD techniques, it is possible to estimate more accurately (up-to several percent) the aerodynamic performances of a particular rotor/propeller in ground effect, including small-scale geometries operating at relatively low Reynolds numbers (Re). Here, low-to-medium Re imply several tens to several hundreds of thousands where transitional flow and laminar separation bubbles (LSBs) may be present. Since these regimes include various flow phenomena, it is best to perform detailed analyses of a particular geometry whenever possible.

Here, a small-scale fixed-pitch propeller/rotor designed for a small quadcopter in hover and in ground effect is numerically investigated. The blade geometry was defined through an optimization study whose details can be found in [7]. Previously mentioned simple semi-empirical relation (based purely on the distance from the ground and rotor size) is complemented by a detailed CFD study. The employed numerical approach (previously tried on an isolated rotor) has been validated through grid convergence study and comparison to available experimental data performed at the University of Belgrade, Faculty of Mechanical Engineering [7]. The propeller, connected to an electric motor, and powered by a battery pack, was mounted on a sliding stand. Thrust was measured by a load cell, whereas power was implicitly estimated from the measured voltage and current.

Few additional explanations should be provided here, before continuing with the details of the current research. The

observed differences in measured and computed thrust were not greater than 15% and were much less for the torque. From numerous numerical studies, differing in complexity and starting assumptions, the authors came to the following conclusions. The differences in the two sets of results are the consequence of several factors. Employing the RANS approach, that completely models and simplifies turbulent motion, contributes up-to 5%. Similarly, medium mesh resolution (comprising several million cells, where geometry is generally well represented, but without extra fine refinement of the leading edge and cells in the wall vicinity) results in approximately 4% error. The greatest contributor to the wrong estimate of thrust seems to come from neglecting the actual experimental set-up, and all the additional objects positioned close to the rotor that may affect its wake, even slightly. That is, "dirty" experimental set-up may contribute around 7-10%. Similarly, if numerical results were to be compared to the wind tunnel data, the effects of its walls should be taken into account, for greater accuracy and reliability of numerical estimation.

So, even though some deficiencies of RANS analyses of this flow phenomena are well-known (and can even be quantified), this is still the most usually employed numerical approach, mostly because of a satisfactory balance between the accuracy of results and computational cost and speed. Also, its credibility (veracity) can be augmented by putting in additional effort into the phases of geometric design, mesh generation and appropriate numerical set-up. With ground effect, we are mostly interested in the increase of thrust at the same power (or decrease of power for the same thrust) in comparison to the performance of an isolated rotor. Therefore, the obtained relative changes (ratios) can be accepted as sufficiently reliable and a good starting point for the estimation of small-scale propeller performances in ground vicinity.

Methodology

Particularities of the employed numerical approach are given below.

Rotor geometry and computational domains

The diameter of the investigated propeller, illustrated in Fig. 1, is $D = 73.2$ cm. Reynolds number based on the chord located at ¾ blade span and at nominal rotational frequency of 3289 rpm is 300,000 (where numerous flow phenomena such as LSB may be expected).
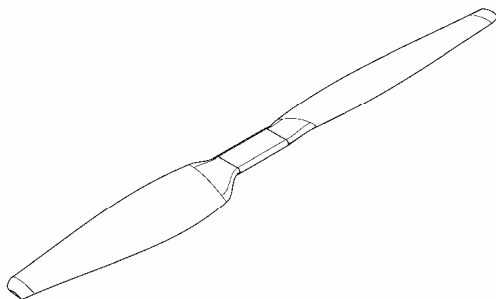

Figure 1. Propeller geometry

Propeller is surrounded by the smaller "rotating" part of the domain, while both parts are located within a much bigger "stationary" zone. In order to appropriately simulate "ground effect", several different outer computational domains had to be modeled, corresponding to the ground distance $z = [0.15$ m, 0.20m, 0.25m, 0.30m, 0.35m, 0.40m, 0.50m], respectively. These values were chosen to adequately capture changes in

thrust. All the outer zones are cylinders of the same outer radius 3.5 m, extending −2 m in upstream, and z to 8 m (for isolated rotor) in downstream direction. In order to achieve some kind of similarity, the inner, "rotating" part of the domain was the same for all models, which means it has to fit into the shortest domain. This cylinder extends from −0.2 m to 0.1 m in streamwise, and 0.6 m in radial direction, respectively.

Computational grids

Likewise, while the "rotor" grid remained the same, different "stator" meshes had to be generated for each considered ground distance z. Overall, all generated grids are sufficiently fine, unstructured hybrid meshes (defined after grid convergence studies). Some details are provided in Figures 2 and 3.
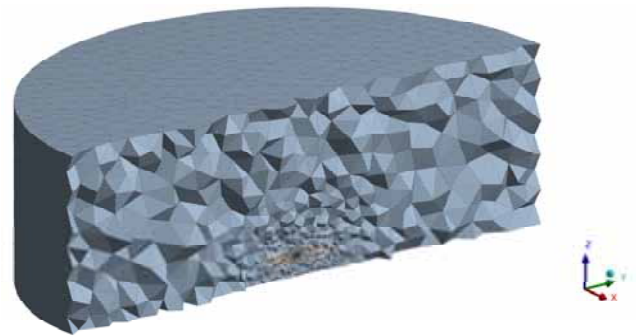

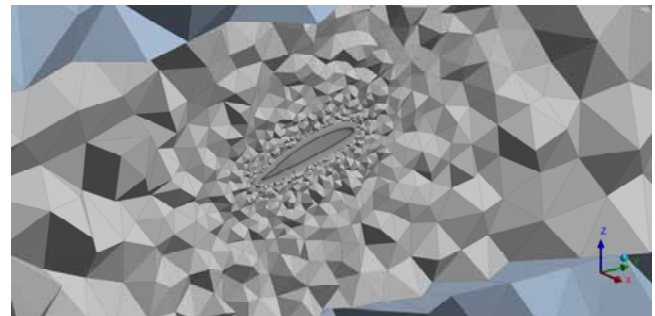**Figure 2.** Cross-section of a generated grid

Figure 3. Detail around the blade

Meshes are additionally refined in close proximity to the propeller that is also encompassed by 25 layers of thin prismatic cells to better capture sudden (quite distinct) changes of flow quantities within the boundary layer. Small differences in the number of cells originate from differences in geometry, but all meshes number from 5.3 to 5.4 million cells (control volumes).

Numerical set-up

The governing RANS equations for 3D, incompressible flows, closed by the $k - \omega$ SST turbulence model, were solved in ANSYS Fluent by the finite volume method. Propeller rotation was accounted for by the quasi-steady multiple reference frames (MRF) approach, where additional terms are simply added to the equations in the "rotating" part of the domain. Even though this is the simplest approach, it gives sufficiently accurate results for statistically steady, nearly axisymmetric flows. Angular velocities close to nominal were assigned to the inner, quasi-rotating zone.

Since hovering condition in ground effect is the main focus of this study, zero values of gauge pressure along the inlet and slip velocity condition along the outlet surface, respectively, are assumed. Blade walls are rotational and no slip. Air is

considered incompressible, and a pressure-based solver is used together with the SIMPLEC pressure-velocity coupling scheme. All spatial discretizations are of the 2nd order. The computations are performed until achieving the convergence of aerodynamic forces and moments (thrust and torque).

Results and Discussion

Computed and approximated increases in thrust, while keeping constant angular velocity and nearly constant torque (and power), are illustrated in Fig.4.
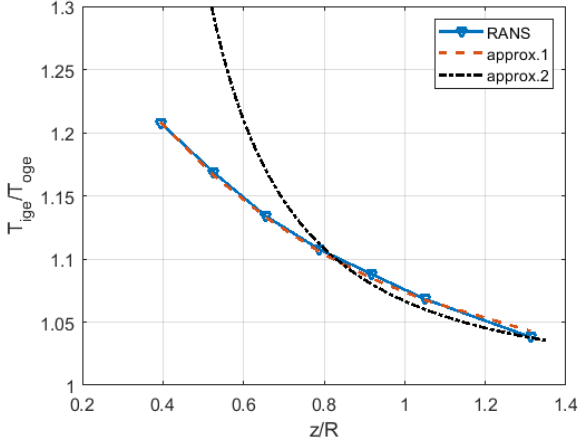

Figure 4. $T_{IGE}/T_{OGE} = f(z/R)$

Approximation 2 is represented by Eq. 1, whereas approximation 1 is derived for this particular propeller geometry, and can be written in the following form:

$$\frac{T_{IGE}}{T_{OGE}} = 1 + 0.41 e^{-1.72\frac{z}{R}} \qquad (2)$$

Although other functions could have been used also, this form was chosen for its asymptotic behavior, i.e. for infinite z, the ratio T_{IGE}/T_{OGE} goes to 1. The approximation proposed here is less steep than the usually employed general semi-empirical relation and gives more realistic estimates for small ground distances ($z/R < 0.8$). At higher ground distances, the two approximations seem sufficiently similar. For more clarity, the values illustrated in Fig.4 are also listed in Table 1.

Table 1. Computed relative changes in thrust for different ground distances

z (m)	z/R	T_{RANS}/T_{OGE}	$T_{approx1}/T_{OGE}$	$T_{approx2}/T_{OGE}$
0.15	0.3937	1.2079	1.2083	1.6757
0.20	0.5249	1.1688	1.1662	1.2933
0.25	0.6562	1.1338	1.1326	1.1698
0.30	0.7874	1.1077	1.1058	1.1121
0.35	0.9186	1.0879	1.0844	1.0800
0.40	1.0499	1.0682	1.0674	1.0601
0.50	1.3123	1.0382	1.0429	1.0377

Similarly, it is possible to make an approximation of the power decrease while keeping constant thrust, which is illustrated in Fig.5. The obtained numerical results indicate that, in ground proximity, the same levels of thrust can be achieved for nearly 30% less power, which can lead to significant savings and prolonged flight endurance.

The novel approximation proposed here, and sketched in Fig.4, can be written as:

$$\frac{P_{IGE}}{P_{OGE}} = 1 - 0.72 e^{-1.58\frac{z}{R}} \qquad (3)$$

Since power required for hover comprises two parts, induced and profile, that account for the air acceleration through the rotor and blade drag, respectively, it is necessary to define a separate approximate expression (Eq. 3), instead of simply using the one for the thrust (Eq. 2) at the power 3/2. Furthermore, the requirement of asymptotic character of the fitting curve is again satisfied. In both cases, the R-square (R^2) of the proposed fits was above 0.995.
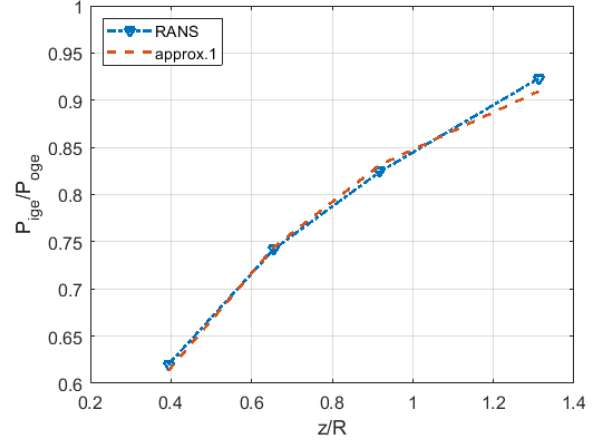

Figure 5. $P_{IGE}/P_{OGE} = f(z/R)$

Ground effect can qualitatively be represented by different flow visualizations. Fig.6 illustrates three different computed fields of induced velocities in mid-plane, for $z = 0.2$ m, $z = 0.5$ m and infinite z (isolated rotor). In all cases, the greatest contributions of the outer blade segments are clearly visible, as well as the nearly non-existing induced velocities around the blade roots. When the outlet boundary is close to the rotor, the streamtube adjusts and slides along it. The wakes shed from the two blades remain distinct and expand outwards. On the other hand, for the isolated rotor, the two wakes merge and the total structure contracts as the flow continues to accelerate downstream.
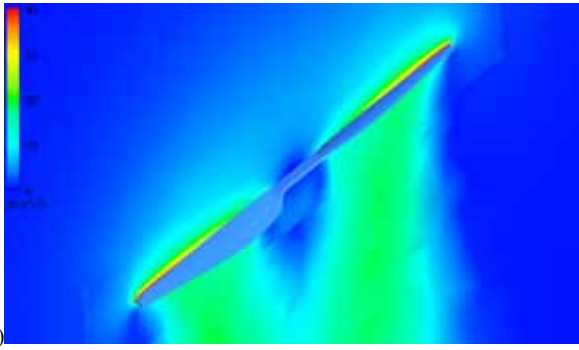
a)

b)
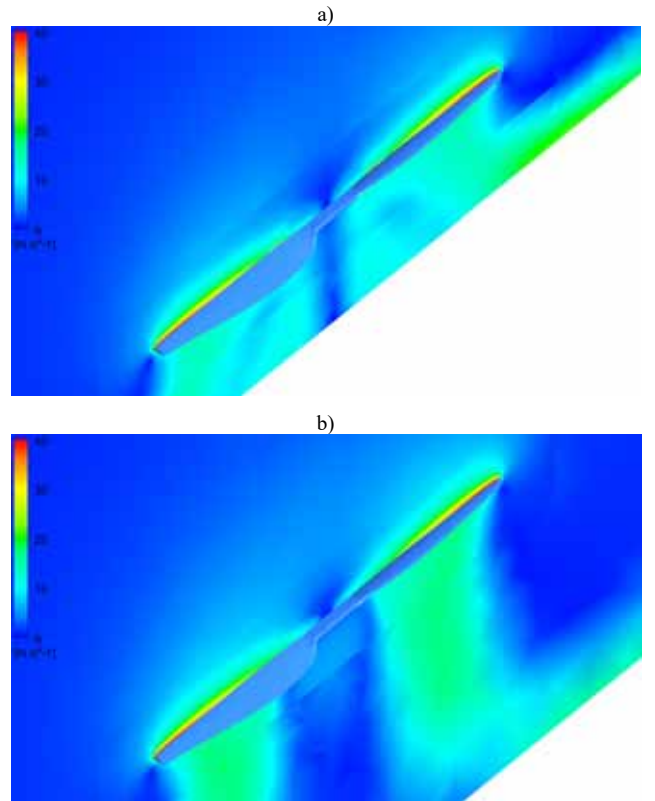
Figure 6. Induced velocities at: a) z = 0.2 m, b) z = 0.5 m, and c) infinite z

It is also possible to compare pressure distributions along the propeller blades for different ground distances, as illustrated in Fig.7. Zones of lower pressure along the upper blade surfaces near the tips seem less affected by the ground vicinity in comparison to the blade root segments, where differences in pressure contours are more visible. The benefits of ground effect are apparently caused by prolonged zones of negative gauge pressure that stretches towards the blade root and leading edge.
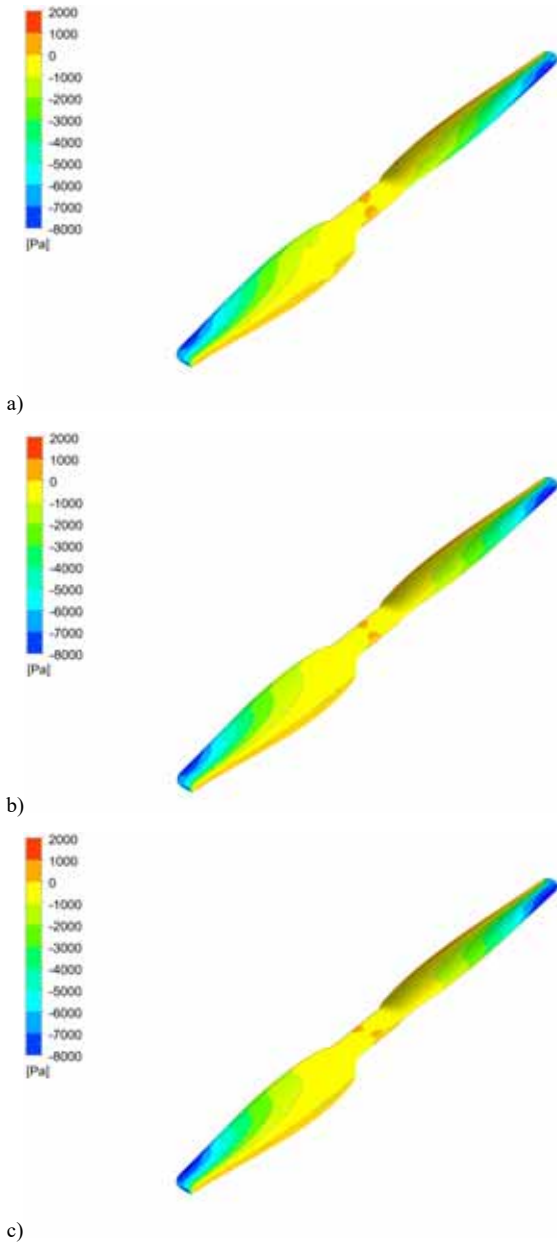

Figure 7. Gauge pressure along the propeller at: a) z = 0.2 m, b) z = 0.5 m, and c) infinite z

These statements can be further validated by inspecting the vortices shed from the blades at different ground distances (Fig.7). Again, tip vortices appear similar in all cases. Primary vortical structures are slightly better differentiated in the case of an isolated rotor and seem to disperse somewhat more quickly if ground surface is relatively close to the rotor. On the other hand, root vortices seem more pronounced as the rotor approaches the ground. At lower distances from the ground z, there seem to be more mixing and instabilities around the central part of the propeller that result in more accelerated air flow. It should be kept in mind, however, that these visualizations directly depend on the way the turbulent motion is resolved.

Most of the general findings presented here match the well-known theoretical models that are usually used for the analysis of rotor performance as well as the numerical results presented in [5].
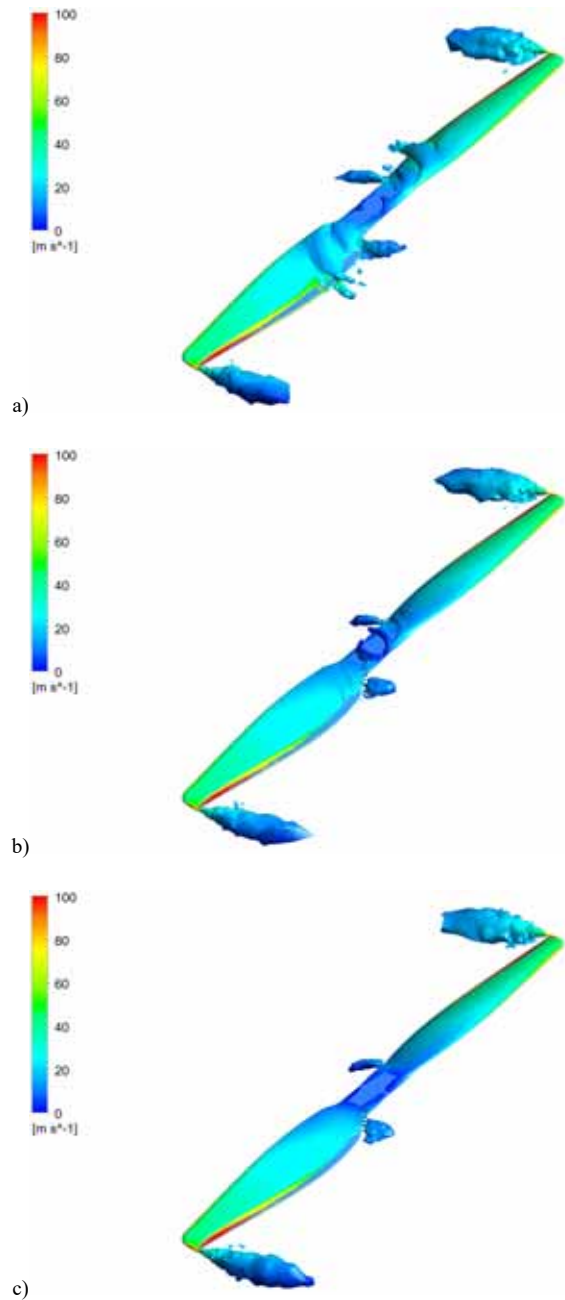

Figure 8. Vortical structures at: a) z = 0.2 m, b) z = 0.5 m, and c) infinite z

Final quantification of different flow behaviour along the blade with respect to ground distance z is provided in Fig.9 by pressure coefficient distributions.
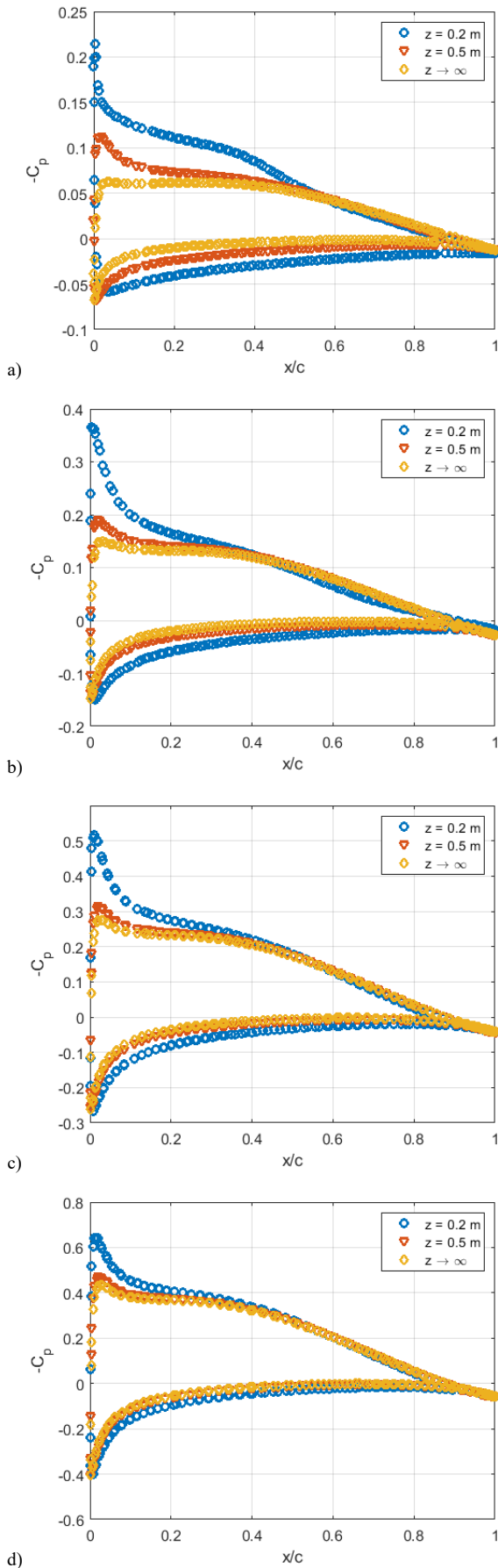
Figure 9. Pressure coefficient distributions in cross-sections located at: a) $y = 0.10$ m, b) $y = 0.15$ m, c) $y = 0.20$ m, and d) $y = 0.25$ m

Pressure coefficient distributions in cross-sections located at 26%, 39%, 52% and 65% blade span clearly indicate that the flows mostly differ in the vicinity of the leading edge, on both the upper and lower blade surfaces.

Conclusions

A fixed-pitch small-scale hovering propeller of a quadcopter (or any delivery UAV) in ground effect was numerically investigated by solving RANS equations for incompressible fluid. Increase of thrust at constant power (and vice versa) with respect to the relative distance from the ground was determined and mathematically formulated. Furthermore, interesting flow visualizations are presented.

Some more particular contributions and findings of this research study are as follows:

- Atypically small distances from the ground were considered,
- Small-scale propeller geometry operating at low Re was analyzed whereas most previous studies were focused on helicopter rotors,
- Novel approximations of changes of thrust and power in ground vicinity are proposed,
- More realistic estimations are obtained for lower ground distances,
- Some important and distinctive flow features are captured, illustrated and discussed.

Although the presented novel relations are derived for a particular propeller geometry, they are also applicable to other "similar" small-scale propellers (of comparable shape, size, and operating conditions). However, the actual sensitivity study of the coefficients appearing in Eqs. 2 and 3 might be the topic of a future study.

Acknowledgement

References

[1] DELORME,Y., STANLY,R., FRANKEL,S.H., GREENBLATT,D.: *Application of Actuator Line Model for Large Eddy Simulation of Rotor Noise Control*, Aerospace Science and Technology, 108 (2021) 106405.

[2] HERNICZEK,M.K., JEE,D., SANDERS,B., FESZTY,R.: *Rotor blade optimization and flight testing of a small UAV rotorcraft*, Journal of Unmanned Vehicle Systems, 7(4) (2019) 325-344.

[3] ZHAO,Q., SHENG,C.: Predictions of HVAB rotor in hover using hybrid RANS/LES methods-II, AIAA SciTech Forum 2022, AIAA 2022-1550.

[4] LEISHMAN,J.G.: *Principles of Helicopter Aerodynamics*, Cambridge University Press, New York, 2006.

[5] GAROFANO-SOLDADO,A., SANCHEZ-CUEVAS,P.J., HEREDIA,G., OLLERO,A.: Numerical-experimental evaluation and modelling of aerodynamic ground effect for small-scale tilted propellers at low Reynolds numbers, Aerospace Science and Technology, 126 (2022) 107625.

[6] COOMBES,M., NEWTON,S., KNOWLES,J., GARMORY,A.: *The influence of rotor downwash on spray distribution under a quadrotor unmanned aerial system*, Computers and Electronics in Agriculture, 196 (2022) 106807.

[7] KOVAČEVIĆ,A., SVORCAN,J., HASAN,M.S., IVANOV,T., JOVANOVIĆ,M.: *Optimal propeller blade design, computation, manufacturing and experimental testing*, Aircraft Engineering and Aerospace Technology, 93(8) (2021) 1323-1332.

Numerička analiza elise u blizini zemlje

Detaljne analize strujnog polja oko elisa dobijaju na značaju širom sveta kako se njihov broj i moguće namene stalno uvećavaju (naročito kod budućih letećih vozila). Dodatna karakteristika elisa za male bespilotne letelice je što one treba da rade u širokom opsegu (donekle netipičnih) radnih uslova koji uključuju let unazad, let u blizini prepreka, čvrstih površina, itd. Ovi specifični zahtevi postavljaju pitanje uticaja zemlje na aerodinamičke performanse elise. U ovom radu numerički su ispitana strujna polja oko male, namenski izrađene elise u blizini zemlje. Različite udaljenosti od površine su razmatrane i nove zavisnosti vučne sile i snage od te udaljenosti su predložene. Da bi se dobili dovoljno pouzdani i tačni rezultati i uhvatile najznačajnije strujne strukture, Navije-Stoksove jednačine osrednjene Rejnoldsovom statistikom su rešene metodom konačnih zapremina. Dodatno su predstavljene najinteresantnije vizuelizacije strujnog polja. Iako se dobijeni trend promene vučne sile dobro uklapa sa uobičajenom polu-empirijskom formulom, realističnije procene su dobijene za manje vrednosti udaljenosti od zemlje. Takođe, pozitivni uticaj blizine zemlje na aerodinamičke performanse rotora su još jednom potvrđene i kvantifikovane

Ključne reči: **elisa, turbulencija, RANS, uticaj zemlje.**